

Computer Methods in Biomechanics and Biomedical Engineering

ISSN: (Print) (Online) Journal homepage: www.tandfonline.com/journals/gcmb20

OpenOFM: an open-source implementation of the multi-segment Oxford Foot Model

Philippe C. Dixon, Elodie E. Drew, Sean P. McBride, Marian Harrington, Julie Stebbins & Amy B. Zavatsky

To cite this article: Philippe C. Dixon, Elodie E. Drew, Sean P. McBride, Marian Harrington, Julie Stebbins & Amy B. Zavatsky (04 Feb 2025): OpenOFM: an open-source implementation of the multi-segment Oxford Foot Model, Computer Methods in Biomechanics and Biomedical Engineering, DOI: [10.1080/10255842.2024.2448558](https://doi.org/10.1080/10255842.2024.2448558)

To link to this article: <https://doi.org/10.1080/10255842.2024.2448558>



© 2025 The Author(s). Published by Informa UK Limited, trading as Taylor & Francis Group



View supplementary material [↗](#)



Published online: 04 Feb 2025.



Submit your article to this journal [↗](#)



Article views: 376








View related articles [↗](#)



View Crossmark data [↗](#)

OpenOFM: an open-source implementation of the multi-segment Oxford Foot Model

Philippe C. Dixon^{a,b,c} , Elodie E. Drew^{b,c,*} , Sean P. McBride^d, Marian Harrington^e , Julie Stebbins^{e,f}  and Amy B. Zavatsky^g 

^aDepartment of Kinesiology and Physical Education, McGill University, Montreal, Canada; ^bSchool of Kinesiology and Physical Education, University of Montreal, Montreal, Canada; ^cAzrieli Research Center of CHU Sainte-Justine, Montreal, Canada; ^dDepartment of Rehabilitation Sciences, Medical University of South Carolina, Charleston, SC, USA; ^eOxford Gait Laboratory, Oxford University Hospitals NHS Foundation Trust, Oxford, United Kingdom; ^fNuffield Department of Orthopaedics, Rheumatology and Musculoskeletal Sciences, University of Oxford, Oxford, United Kingdom; ^gDepartment of Engineering Science, University of Oxford, Oxford, United Kingdom

ABSTRACT

The Oxford Foot Model (OFM) is a widely-used multi-segment foot model for the evaluation of foot motion. To date, custom code based on the original scientific publications have failed to reproduce results available through the Vicon plug-in (ViconOFM). This highlights a lack of transparency, affecting the accessibility and understanding of the model. Therefore, the aims of this study are to (1) replicate ViconOFM using Python for open-source distribution (openOFM v1.0) and (2) reproduce the original scientific description of the OFM in a second version (openOFM v1.1), highlighting differences between both versions. A dataset comprising one healthy adult and a set of five patients with heterogeneous foot pathologies was used for analyses. Evaluation was conducted using the normalised root mean square error (NRMSE) between the inter-segment angles and arch heights of both implementations. The openOFM v1.1 was developed based on the original OFM publications. The average NRMSE between ViconOFM and openOFM v1.0, using both healthy and pathological gait, was of 0.0012. Based on our openOFM v1.1 implementation, differences between ViconOFM and the original OFM description from the literature are due to an integrated smoothing and gap filling function and changes in segment definitions. The negligible differences between ViconOFM and openOFM v1.0 in healthy and pathological gait supports the concurrent validity of openOFM. Providing users with both openOFM versions enables informed use of either model and allows further investigation into the implications of these differences. The open-source nature of the project promotes further development.

HIGHLIGHTS

- Modelling foot movement is a complex task requiring methodological transparency
- The Oxford Foot Model (OFM) is only accessible within commercial software (Vicon)
- Open-source code for the OFM (openOFM) was developed and validated
- Differences were found between Vicon OFM and the OFM descriptions in literature
- openOFM addresses these differences and provides a platform for future development

ARTICLE HISTORY

Received 17 August 2024
Accepted 26 December 2024


KEYWORDS

Multi-segment; Vicon; kinematics; intra-foot; foot modelling


1. Introduction

The foot is an intricate structure with complex anatomy, facilitating stable and efficient gait. In cases of foot deformity, gait analysis can quantify dynamic problems and help improve the surgical decision making process (Fuller et al. 2002); however, standard single-segment biomechanical foot models can result

in misinterpretation of foot function (Pothrat et al., 2015). To overcome this limitation, multi-segment foot models (MSFMs), capable of measuring subtle foot movements, have been developed (Leardini et al., 2019). The most-widely used MSFMs for analysis of foot deformities (Leardini et al., 2019) are the Oxford Foot Model (OFM) (Stebbins et al. 2006), the Rizzoli Foot

CONTACT Philippe C. Dixon  phil.dixon@mcgill.ca

*Co-first author

 Supplemental data for this article can be accessed online at <https://doi.org/10.1080/10255842.2024.2448558>.

© 2025 The Author(s). Published by Informa UK Limited, trading as Taylor & Francis Group
This is an Open Access article distributed under the terms of the Creative Commons Attribution License (<http://creativecommons.org/licenses/by/4.0/>), which permits unrestricted use, distribution, and reproduction in any medium, provided the original work is properly cited. The terms on which this article has been published allow the posting of the Accepted Manuscript in a repository by the author(s) or with their consent.

Model (Leardini et al. 2007), and the Milwaukee Foot Model (Kidder et al., 1996). Most recently, the Amsterdam Foot Model, designed to minimize errors due to soft tissue movement and marker misplacement, was developed (Schallig et al. 2022). Each of these models comprise tibia, hindfoot, forefoot, and hallux segments; allowing for computation of three-dimensional intra-foot segment kinematics, with the Rizzoli Foot Model and Amsterdam Foot Model also including a midfoot segment.

The OFM has been particularly popular due to its inclusion as a plug-in for commercial software since 2005, although its development began in 2001 with the publication of a first article stemming from the evaluation of hallux motion (Carson et al. 2001). In 2006, a second article was published, introducing modifications to the tibia and forefoot definitions (Stebbins et al. 2006). Notably, the model was modified for compatibility with the popular Plug-in Gait lower-limb model (Kadaba et al. 1990), available through the Vicon software. This publication is the basis for the commercial implementation of the OFM in Vicon Nexus.

Despite the relatively long history of the OFM, certain problems limit more widespread implementation. Notably, Schallig et al. (Schallig et al. 2020), reported that custom-made scripts based on published OFM definitions were unable to replicate the joint kinematics computed from Vicon Nexus software pipelines. Given the importance of reproduction in research (Mesirov 2010), sharing source code when publishing a biomechanical model, as was done for the Amsterdam Foot Model (Schallig et al. 2022), is worthwhile. Previous open-source projects replicating the Plug-in Gait model (first pyCGM (Schwartz and Dixon 2018) in 2018 and pyCGM2 (Leboeuf et al. 2019)), have allowed the biomechanics community to work towards substantial improvements in lower-limb modelling. Increased transparency surrounding the OFM through open-source model development is therefore crucial. Here, we focus on two practical, inter-related, issues of the OFM, a model for which our team has extensive research and clinical experience. First, the model is currently implemented as an executable ('closed') plug-in within commercial software, making code inspection impossible. Transparency in computational methods is necessary to ensure reproducible research (Mesirov 2010). An open-source alternative would remove barriers, allowing code inspection and improvement. Second, limited mathematical details are available in published papers making replication of MSFMs difficult (Bishop

et al. 2012). A complete mathematical description of the OFM is essential to help the biomechanics community gain confidence in the model and promote further developments.

Thus, the aims of this study are to (1) replicate the OFM as implemented in the Vicon Nexus software (Vicon, Oxford Metrics Inc., Oxford, UK) plug-in using an open-source programming language and (2) identify and address inconsistencies between the existing Vicon implementation and original descriptions provided in Carson et al. (Carson et al. 2001) and Stebbins et al. (Stebbins et al. 2006). These aims will be reflected in our code as version 1.0 ('Legacy') and version 1.1 ('as described'), respectively. Code is validated using a dataset comprising one healthy participant and five patients with heterogeneous foot pathologies and released as the openOFM project in a public code repository.

To ensure the first aim of this project is attained, the following criteria must be met: accurate reproduction of the OFM results from the commercial implementation (validation), complete transparency of the openOFM method, and full accessibility of the final code. Validation is accomplished by measuring differences between the openOFM and commercial OFM using the normalised root mean square error (NRMSE), normalised to the magnitude of the commercial OFM results. Transparency is achieved through a detailed description of our computational methods in the present paper accompanied by our publicly available code and validation data on GitHub. To maintain the highest level of accessibility, the programming language selected for the openOFM is Python, a free general purpose programming language highly rated for code readability (Ahmed et al. 2021). Nonetheless, Matlab (The Mathworks Inc., Natick, USA) code is also provided.

To ensure the second aim of this project is attained, version 1.1 must implement the OFM as described by Carson et al. (Carson et al. 2001) in 2001 and Stebbins et al. (Stebbins et al. 2006) in 2006.

2. Materials & methods

The OFM has been described elsewhere (Carson et al. 2001; Stebbins et al. 2006); however, to date, a complete mathematical description has not been presented. We now provide sufficient detail for implementation of the model in open-source form as openOFM versions 1.0 and 1.1. General notation used herein is summarized in Table 1. Following a short summary of the participant data used in this paper,

this section provides a comprehensive description of the markers whose trajectories are input to the OFM. Next, segment definitions are outlined, along with kinematic and arch height calculations. Finally, the process for model implementation is presented.

2.1. Participant data

The validation of the openOFM with respect to the Vicon Nexus implementation is conducted using a dataset comprised of a single walking trial from a healthy adult and a heterogeneous dataset of 5 patients with various foot pathologies extracted from the Oxford Gait Laboratory database. Patients were selected to ensure a wide range of gait patterns. Demographic information is summarized in Table 2. All patients provided consent for their gait data to be used in future research studies. The steps followed to process the data are presented in detail in Supplementary Appendix E.

2.2. Markers

Inputs to the OFM are the three-dimensional trajectories of points on the lower leg and foot (Figure 1, Table 3) identified by retro-reflective markers attached to the skin. Their positions are tracked by a motion capture system in a laboratory-based (fixed) reference frame defined by a global coordinate system. These physical markers are split into two categories: ‘tracking’ markers remain in place during all data capture trials, and ‘static’ markers are removed after their positions are measured in a static trial, in which

the subject adopts a posture as close to neutral as possible (anatomical position).

Markers are used to define two sets of local, segment-embedded (moving) coordinate systems: ‘technical’ frames are used to specify a segment’s position and orientation in space using physical markers (Supplementary Appendix A), while ‘anatomical’ frames are related to anatomical landmarks, directions, and planes, and their definition may require additional points. Here, these additional points are referred to as ‘virtual’ markers and are defined in the OFM as indicated in Figure 1 and Table 4.

2.2.1. Virtual markers

A virtual marker refers to any point used by the model that does not correspond to a physical marker tracked by the motion capture system. Its location can be derived directly from the position of at least two other markers (derived marker), or defined relative to the technical frames of the segments in the static trial (technical marker) and move with the technical frames in the dynamic trials. Static markers, which are removed during dynamic trials and tracked relative to the technical frame, are also considered virtual markers in dynamic trials. Using these markers, the anatomical frames can be defined during movement.

The location of certain virtual markers are impacted by two optional settings in the OFM; *Hindfoot Flat* (Section 2.2.4) and *Forefoot Flat* (Section 2.2.5). They can be used to ensure the hindfoot and forefoot longitudinal axes are parallel to the floor; however, they are not substitutes for careful marker placement.

2.2.2. Replacing missing marker frames

In the original description of the OFM, a function in Vicon’s Bodybuilder (Vicon, 2010) scripting language was used to estimate the position of missing markers based on the position of three other markers on the same rigid segment (Stebbins et al. 2006). This *replace4* [17] function also had a desirable smoothing

Table 1. Nomenclature.

Notation	Definition
XYZ	Global, laboratory (fixed) coordinate reference frame
xyz	Local, segment-based (moving) coordinate reference frame
$\hat{i}, \hat{j}, \hat{k}$	Unit vectors of the xyz coordinate system
\mathbf{r}_a	Position vector of point a
TB	Tibia segment
HF	Hindfoot segment
FF	Forefoot segment
HX	Hallux segment

Table 2. Patient demographic and processing settings.

Label	Diagnosis	Age	Foot deformity (Right/Left)	Hindfoot flat	Forefoot flat
H	Healthy	24.0	N/A	Both	Both
P1	Hemiplegia (L)	50.8	Neutral/Equinus.	Right	None
P2	Spastic diplegia	13.5	Planovalgus/Planovalgus	Left	None
P3	Hemiplegia (R)	49.3	Planus/Planus	Both	None
P4	Toe walk	12.4	Equinovarus, FF add/Equinovarus, FF add	None	None
P5	Toe walk	27.2	FF add/HF varus, FF add	None	None
P6	Intoeing	20.1	Neutral/Neutral	None	None

Abbreviations: Adduction (add), Forefoot (FF), Hindfoot (HF), Left (L), Right (R).

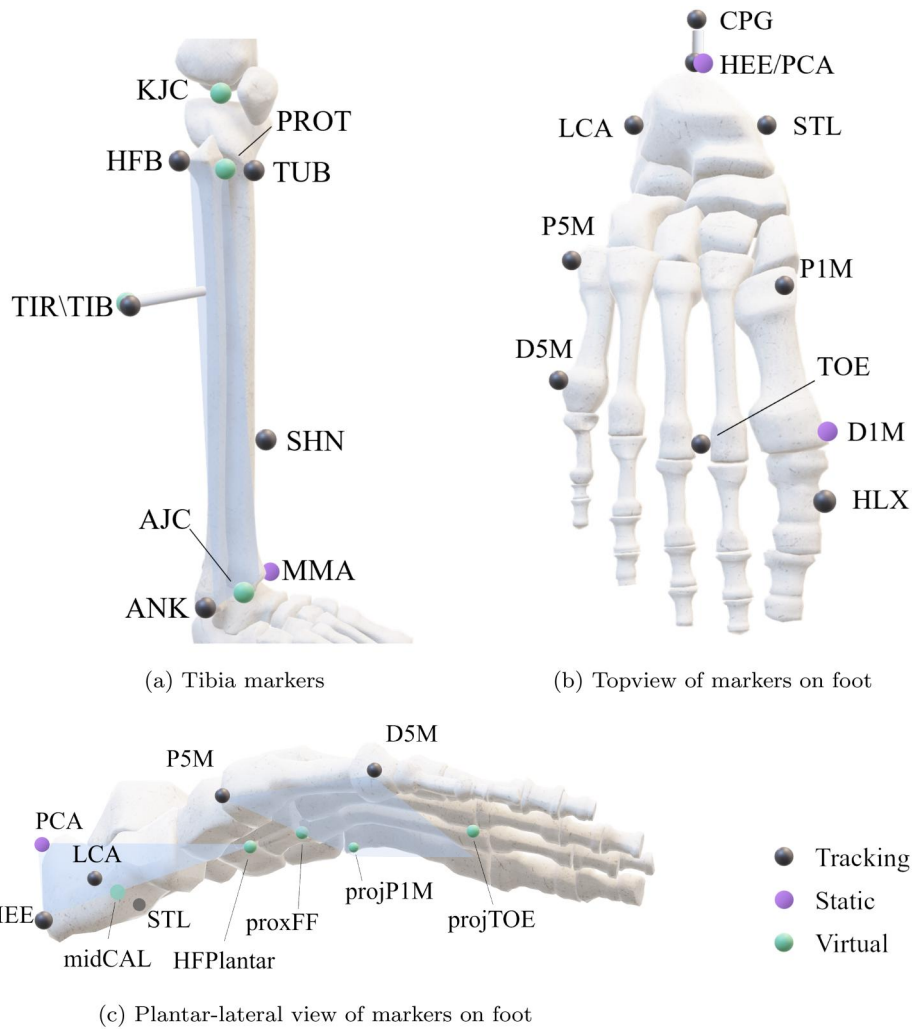


Figure 1. The physical tracking and static markers (black, purple), as well as virtual (green) markers, for the tibia (a), and foot (b, c). The bone anatomy images were created using Powerpoint (Microsoft Inc., Redmond, USA).

Table 3. Oxford foot model physical marker labels and location.

Segment	Label	Location
Tibia	HFB	Head of fibula
	TIB	Wand marker on lateral aspect of tibia
	TUB	Most anterior aspect of tibial tuberosity
	SHN	Anywhere along the linear alba of tibia
	ANK	Most lateral aspect of lateral malleolus
	MMA	Most medial aspect of medial malleolus
Hindfoot	HEE	Posterior distal end of calcaneus in midline
	PCA	Posterior proximal end of calcaneus in midline
	CPG	Wand marker, placed between HEE and PCA
	STL	Medial calcaneus on sustentaculum tali
	LCA	Lateral calcaneus ^a
Forefoot	P1M	Base of 1st metatarsal ^b
	D1M	Medial aspect of head of first metatarsal
	P5M	Lateral to base of 5th metatarsal
	D5M	Lateral aspect of head of 5th metatarsal
	TOE	Between heads of 2nd and 3rd metatarsals
Hallux	HLX	Base of the medial aspect of the hallux

Marker abbreviations as implemented in Vicon. See references (Carson et al. 2001; Stebbins et al. 2006) for original nomenclature. Markers in italics are used in the static trial only and are removed for dynamic trials. (a) Placed at same height and antero-posterior distance from HEE as STL, (b) medial to extensor hallucis longus tendon.

effect, improving the repeatability of results by removing occasional and unpredictable spikes due to noise, and was therefore applied to all OFM markers in the tibia, hindfoot, and forefoot. The effect of this process is analysed in Section 4.4. In v1.1, this function is removed.

2.2.3. Tibia

The ANK, HFB and SHN physical markers listed in Table 3 are used to define the tibial technical frame. There are five virtual markers used to define the two tibial anatomical frames, described in Section 2.3.2. These are the rotated TIB marker (TIR), the knee joint center (KJC), the ankle joint center (AJC), PROT, and the mid-malleolar point (midMAL). The TIR, KJC, and AJC virtual markers are inherited from the Plug-in-Gait model and are defined in Vicon Nexus documentation (Lower body kinematics - Nexus 2.16 documentation 2024). The PROT marker is the projection of TUB on the plane

Table 4. Oxford foot model virtual marker labels and location.

Segment	Label	Location
Tibia	TIR	Rotated TIB marker
	KJC	Plug-in-gait knee joint centre
	AJC	Plug-in-gait ankle joint centre
	PROT	Projection of TUB marker on mid-frontal plane of tibia
	midMAL	Mid-point of line segment connecting malleoli (ANK and MMA)
Hindfoot	midCAL	Mid-point of line segment connecting LCA and STL
Forefoot	HFPlantar	Projection of P5M on the hindfoot mid-sagittal plane, adjusted to the height of HEE if hindfoot flat
	projTOE	Projection of TOE on the forefoot transverse plane
	projP1M	Projection of P1M on the forefoot transverse plane
	proxFF	Mid-point of projP1M and P5M

Marker abbreviations as implemented in Vicon. See (Carson et al. 2001; Stebbins et al. 2006) for original nomenclature.

defined by MMA, ANK, and HFB, calculated as described in [Supplementary Appendix C.2](#).

2.2.4. Hindfoot

The HEE, STL, and LCA markers are used to define a technical frame. The hindfoot anatomical frame requires two additional virtual markers: midCAL and HFPlantar. MidCAL is the STL-LCA mid-point. HFPlantar is the projection of the P5M marker onto the mid-sagittal plane as described in [Supplementary Appendix C.2](#) using the midCAL, PCA, and HEE markers.

The *Hindfoot Flat* option can be used if the hindfoot is on the floor during the static calibration pose to force the segment's longitudinal axis parallel to the floor. This is achieved by making the height of HFPlantar equal to the height of HEE.

In v1.1, a modification is introduced to reduce the sensitivity of the hindfoot's longitudinal (antero-posterior) axis to changes in varus/valgus alignment when the *Hindfoot Flat* option is used ([Section 4.4](#)). The HFPlantar definition is modified such that it lies at the intersection of the mid-sagittal plane (described above), and a plane parallel to the floor, at the height of HEE. Details can be found in [Supplementary Appendix C.3](#).

2.2.5. Forefoot

The P1M, D1M, P5M and D5M physical markers listed in [Table 3](#) are used to define the forefoot technical frame.

A virtual D1M marker is created in dynamic trials from its position with respect to the technical frame in the static trial. The plantar surface of the forefoot is then defined by the plane containing P5M, D5M and D1M. The P1M and TOE markers are projected into this plane to obtain projP1M and projTOE, respectively. A proximal forefoot point (proxFF) is then defined as the mid-point between projP1M and P5M (accounting for marker diameter), according to Equations C15 and C14.

If the forefoot flat option (*Forefoot Flat*) is used, the height of D1M and D5M is made equal to the height of P5M. Reliance on this option is discouraged, as the D1M, D5M, and P5M markers should be placed on the foot at the same height from the plantar surface of the forefoot. *Forefoot Flat* will not be supported in future versions.

2.3. Segments

The tibia (TB), hindfoot (HF), forefoot (FF), and hallux (HX) segments are now defined.

2.3.1. General definition

The anatomical frame is representative of the subject-specific segment anatomy ([Figure 2](#)) and is used to calculate inter-segment kinematics. Each anatomical frame is constructed based on the coordinates of at least three points. The anatomical directions (antero-posterior, medial-lateral, proximal-distal) are approximated from these points.

First, the origin of the segment, O_{seg} , is defined as a point P_1 . Next, the first axis to be calculated, \hat{a}_1 , is a unit vector between O_{seg} and an anatomically relevant proximal or distal point (P_2) representing the long axis of a bone or segment:

$$\hat{a}_1 = \frac{\mathbf{r}_{P_2} - \mathbf{r}_{P_1}}{|\mathbf{r}_{P_2} - \mathbf{r}_{P_1}|} \quad (1)$$

In the openOFM, \hat{a}_1 is positive in the distal direction, with the exception of the tibia segment, where it is positive proximally ([Figure 2](#)). The second axis, \hat{a}_2 , is perpendicular to \hat{a}_1 , and a temporary vector \mathbf{r}_v :

$$\hat{a}_2 = \frac{\mathbf{r}_v \times \hat{a}_1}{|\mathbf{r}_v \times \hat{a}_1|} \quad (2)$$

where

$$\mathbf{r}_v = (\mathbf{r}_{P_3} - \mathbf{r}_{P_4}) \quad (3)$$

The third axis, \hat{a}_3 , is perpendicular to the previous two axes, such that the right-hand rule is followed.

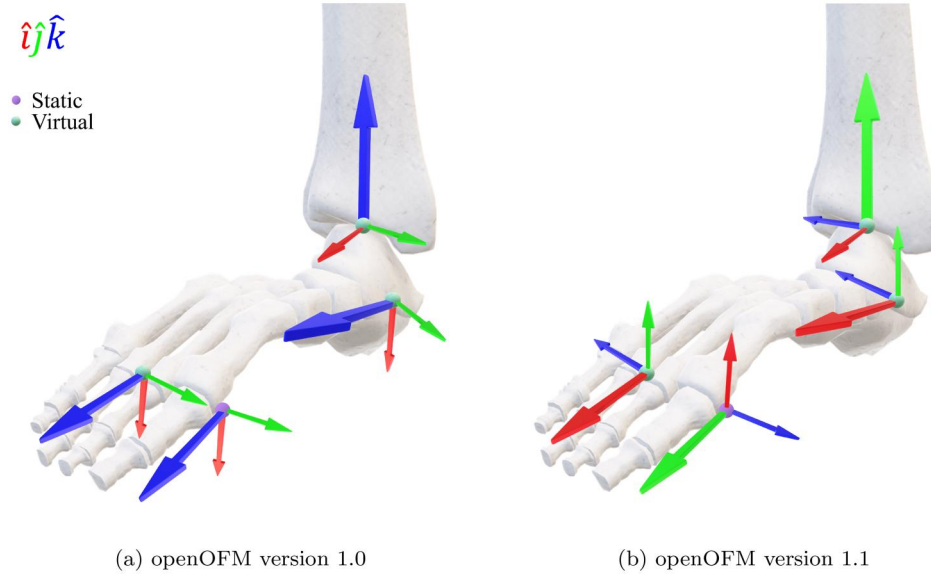


Figure 2. The segment-embedded coordinate systems for each segment in (a) version 1.0 and in (b) version 1.1. Axes are shown for the right foot only. The right hand rule is preserved on the left side with the implication that if an axis is positive medially in a right foot, it is positive laterally in a left foot, and vice versa. The first axes calculated are highlighted with larger arrows. The bone anatomy images were created using Powerpoint (Microsoft Inc., Redmond, USA).

Table 5. Markers used for OFM segment definitions in versions 1.0 and 1.1.

	Tibia	TibiaLab	Tibia v1.1	Hindfoot	Forefoot	Hallux	Hallux v1.1
P ₁	AJC	midMAL	AnkleJC	HEE	proxFF	D1M	D1M
P ₂	KJC	PROT	KneeJC	HFPlantar	projTOE	HLX	HLX
P ₃	AJC	MMA	MMA	PCA	D1M	D1M	FOF₃
P ₄	TIR	ANK	ANK	HEE	D5M	D5M	projTOE

Segment definition described in [Section 2.3.1](#). Modifications in v1.1 shown in bold font. The FOF₃ virtual marker is used to track the direction of the fore-foot medio-lateral (z_{FF}) axis.

This can result in one of the two following equations, dependent on the relative orientations of the axes:

$$\hat{a}_3 = \hat{a}_1 \times \hat{a}_2 \quad (4)$$

$$\hat{a}_3 = \hat{a}_2 \times \hat{a}_1 \quad (5)$$

The points defining each anatomical frame are presented in [Table 5](#), and the assignment of the \hat{a}_1 , \hat{a}_2 , and \hat{a}_3 vectors to the $\hat{i}\hat{j}\hat{k}$ unit vectors of each segment's anatomical frame is given in [Table 6](#).

In v1.1 the labels and orientation of all segment axes are modified ([Figure 2](#), [Table 6](#)), for increased consistency with the original description of OFM ([Stebbins et al. 2006](#)) and other foot models ([Leardini et al. 2007](#); [Schallig et al. 2022](#)).

2.3.2. Tibia

The TB segment is composed of the tibia and fibula, assumed to move together as a single rigid body. There are two distinct definitions of this segment. *Tibia* is the Plug-in Gait tibia definition, and is used to estimate inter-segment kinematics with the hind-foot (HF) and forefoot (FF). These angles are

therefore sensitive to the use of parameters originating from the Plug-in Gait, described in 2.2.3. A second tibia segment, *TibiaLab*, is used to estimate the kinematics of the tibia relative to the laboratory reference frame, independently from the Plug-In Gait joint centres. It is a relic from the original description of the OFM in 2001 ([Carson et al. 2001](#)), when capture volumes were smaller with lower resolution.

In the *Tibia* segment, the orientations of the anatomical planes and coordinate axes are based on the vector from the AJC to the KJC, as defined by the Plug-in-Gait model, and the vector from AJC to TIR. This definition relies on a rotation offset based on a tibial rotation measure (angle between the knee and trans-malleolar axes in the transverse plane). This aims to define a tibial coronal plane as the plane containing the trans-malleolar axis and knee joint centre. In the *TibiaLab* segment, the coordinate system axes are defined by the vector from midMAL to PROT and the vector from ANK to MMA (trans-malleolar axis).

In v1.1, the two definitions of the TB segment (*Tibia*, *TibiaLab*) are replaced by a single definition.

The segment is defined by a given ankle joint centre (AnkleJC) and a generic knee joint centre (KneeJC), and the trans-malleolar axes (ANK to MMA) (Table 5). If no AnkleJC or KneeJC marker exists in the file being processed, they are defined by default as midMAL and PROT respectively. This allows the use of the openOFM without any additional markers, while still allowing consistent comparisons.

2.3.3. Hindfoot

The HF segment comprises the calcaneus and talus bones. Motions of the talocrural and sub-talar joints are considered to contribute jointly to the motion of the HF segment. The HF segment anatomical planes and coordinate axes are defined by the mid-sagittal plane of the calcaneus in a standing posture, itself defined by the PCA, HEE, midCAL, and HFPlantar (Section 2.2.4).

2.3.4. Forefoot

The FF segment comprises the five metatarsals. The FF segment anatomical planes and coordinate axes are defined by the plantar surface of the forefoot and the proximal mid-point of the forefoot (Section 2.2.5). The antero-posterior axis is defined from proxFF to projTOE.

2.3.5. Hallux

The HX segment is defined by a longitudinal axis, assumed parallel to the long axis of the hallux, from the D1M to HLX markers. In v1.0, the second axis is

defined using the vector from D1M to D5M. In v1.1, the superior-inferior hallux axis, is defined such that it is mutually perpendicular to the hallux longitudinal axis (antero-posterior) and the forefoot medio-lateral axis. This results in angles in the sagittal and transverse plane consistent with the previous definition, while ensuring no calculated internal-external rotation of the hallux in the frontal plane. This is done to avoid any chance of clinical misinterpretation.

2.4. Angular kinematics

The segment-embedded axes described in Section 2.3 are used to calculate the joint kinematics according to the Grood and Suntay approach (c.f. Equations (2a, 2b, 2c, and 3) in (Grood and Suntay 1983)). There are four inter-segment angles defined in the OFM: the HF relative to the TB (HF/TB), the FF relative to the HF (FF/HF), the FF relative to the TB (FF/TB), and the HX relative to the FF (HX/FF). A summary of these angles is presented in Table 7. The TB relative to the laboratory frame is also calculated. A detailed description of the kinematic calculations is found in Supplementary Appendix B.

2.5. Arch height

An indication of arch height is provided in the commercial implementation, and is therefore implemented in openOFM. It is expressed as a percentage of the foot length, measured as the distance from the HEE marker to TOE marker (Supplementary Appendix C.5).

2.6. Implementation

2.6.1. Pre-processing

All data were collected using a Vicon Nexus system. Static trials were reconstructed in Nexus, and labelled manually. They were then saved as *static.c3d* files in

Table 6. Axis labels for each segment in version 1.0 and v1.1.

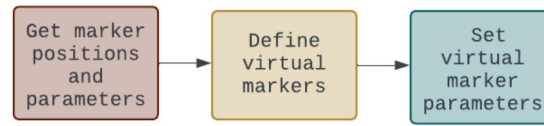
	Tibia		Hindfoot		Forefoot		Hallux	
	v1.0	v1.1	v1.0	v1.1	v1.0	v1.1	v1.0	v1.1
\hat{a}_1	\hat{k}	\hat{j}	\hat{k}	\hat{i}	\hat{k}	\hat{i}	\hat{k}	\hat{j}
\hat{a}_2	\hat{i}	\hat{i}	\hat{j}	\hat{k}	\hat{i}	\hat{j}	\hat{i}	\hat{i}
\hat{a}_3	\hat{j}	\hat{k}	\hat{i}	\hat{j}	\hat{j}	\hat{k}	\hat{j}	\hat{k}

Tibia and *TibiaLab* follow the same sequence.

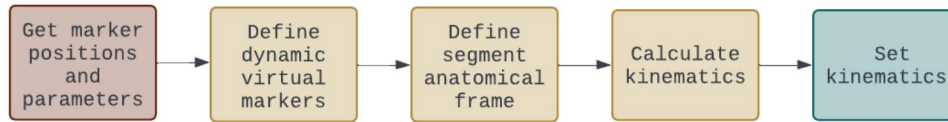
Table 7. Summary of angles for each inter-segment pair.

Plane	Hindfoot/Tibia	Forefoot/Tibia	Forefoot/Hindfoot	Hallux/Forefoot
Sagittal	Dorsi/Plan: Rotate around: v1.0 \hat{j}_{TB} v1.1 \hat{k}_{TB}	Dorsi/Plan: Rotate around: v1.0 \hat{j}_{TB} v1.1 \hat{k}_{TB}	Dorsi/Plan: Rotate around: v1.0 \hat{j}_{HF} v1.1 \hat{k}_{HF}	Dorsi/Plan: Rotate around: v1.0 \hat{j}_{FF} v1.1 \hat{k}_{FF}
Coronal	Inv/Eve: Rotate around: v1.0 \hat{k}_{HF} v1.1 \hat{i}_{HF}	Sup/Pro: Rotate around: v1.0 \hat{k}_{FF} v1.1 \hat{i}_{FF}	Sup/Pro: Rotate around: v1.0 \hat{k}_{FF} v1.1 \hat{i}_{FF}	Int/Ext rotation Rotate around: v1.0 \hat{k}_{HX} N/A
Transverse	Int/Ext rotation: Rotate around: v1.0 <i>floating</i> v1.1 <i>floating</i>	Add/Abd: Rotate around: v1.0 <i>floating</i> v1.1 <i>floating</i>	Add/Abd: Rotate around: v1.0 <i>floating</i> v1.1 <i>floating</i>	Add/Abd: Rotate around: v1.0 <i>floating</i> v1.1 \hat{i}_{HX}

Anatomical terms used to refer to each angle shown in bold. Dorsiflexion/Plantarflexion (Dorsi/Plan), inversion/eversion (Inv/Eve), supination/pronation (Sup/Pro), Internal/External (Int/Ext) rotation, Adduction/Abduction (Add/Abd). The axis around which each angle takes place is also shown for v1.0 and v1.1.



(a) Static processing



(b) Dynamic processing

Figure 3. The general flowcharts for the static and dynamic processing scripts provided with the openOFM.

their subject specific folders. The static trials were then processed using the *Static Oxford Foot Model* plugin provided with Nexus, and saved as *static_processed.c3d* files. Dynamic trials were reconstructed, manually labelled, gaps in marker trajectories were filled following Nexus guidelines, and the trajectories were filtered using the Woltring filter used in the *Dynamic Oxford Foot Model* pipeline. They were then saved as *dynamic.c3d* files in their subject-specific folders. The dynamic trials were then processed using the *Dynamic Oxford Foot Model* Nexus plugin without gap filling or filtering, and saved as *dynamic_processed.c3d* files.

2.6.2. File structure

The openOFM project is split into six subfolders, containing documentation, data, and code for version 1.0 and 1.1. The code for the Matlab implementation of the models is located in the *Matlab* folder and the Python implementation is in the *Python* folder. The Matlab implementation will not be actively supported. The Python code can also be implemented through Vicron Nexus.

Sample data are stored in the *Data_Validate* folder and contains the data used for model validation. Within this folder, *.c3d* files are split into their respective ‘subject’ folders, labelled as either ‘static’ or ‘dynamic’ files.

2.6.3. Program structure

The heart of the openOFM is found in the *OFM* folder of each program folder and contains the main functions used to define virtual marker positions, segments, and inter-segment kinematics. These functions rely on support functions, found in the *utils* and *linear algebra* folders. In Python, basic packages for numerical

computation and file processing are required, as well as the *ezc3d* package (Michaud and Begon 2021) available on GitHub for *.c3d* reading and writing.

The Vicron commercial implementation is composed of two Nexus plugins, *Static Oxford Foot Model* and *Dynamic Oxford Foot Model*. To maintain a similar workflow, the openOFM has two processing functions called *openOFM_static* (Figure 3(a)) and *openOFM_dynamic* (Figure 3(b)) which can be run independently.

Additionally, a processing function is also provided for model validation; *openOFM_validation*. This function automatically runs through a single unprocessed static trial (*static.c3d*) and unprocessed dynamic trial (*dynamic.c3d*) for all subjects in the *Data_Validate* folder. The inter-segment angles obtained are then plotted against the angles from the dynamic trial processed in Vicron Nexus (*dynamic_processed.c3d*) for each subject, with the NRMSE for each set of angles provided.

2.6.4. Options

The OFM offers two processing settings presented earlier, the *Hindfoot Flat* and *Forefoot Flat* (Sections 2.2.4 and 2.2.5, respectively). These are set by the *HFFlat* and *UseFloorFF* parameters, respectively, and are also implemented in the openOFM. They are set as either *True* or *False* for the right and left sides separately during static trial processing. All subsequent dynamic trials have the same settings.

The openOFM can reproduce the commercial implementation of the OFM, as version 1.0, or as it was originally described (Stebbins et al. 2006) as version 1.1. This is done by modifying the *version* argument.

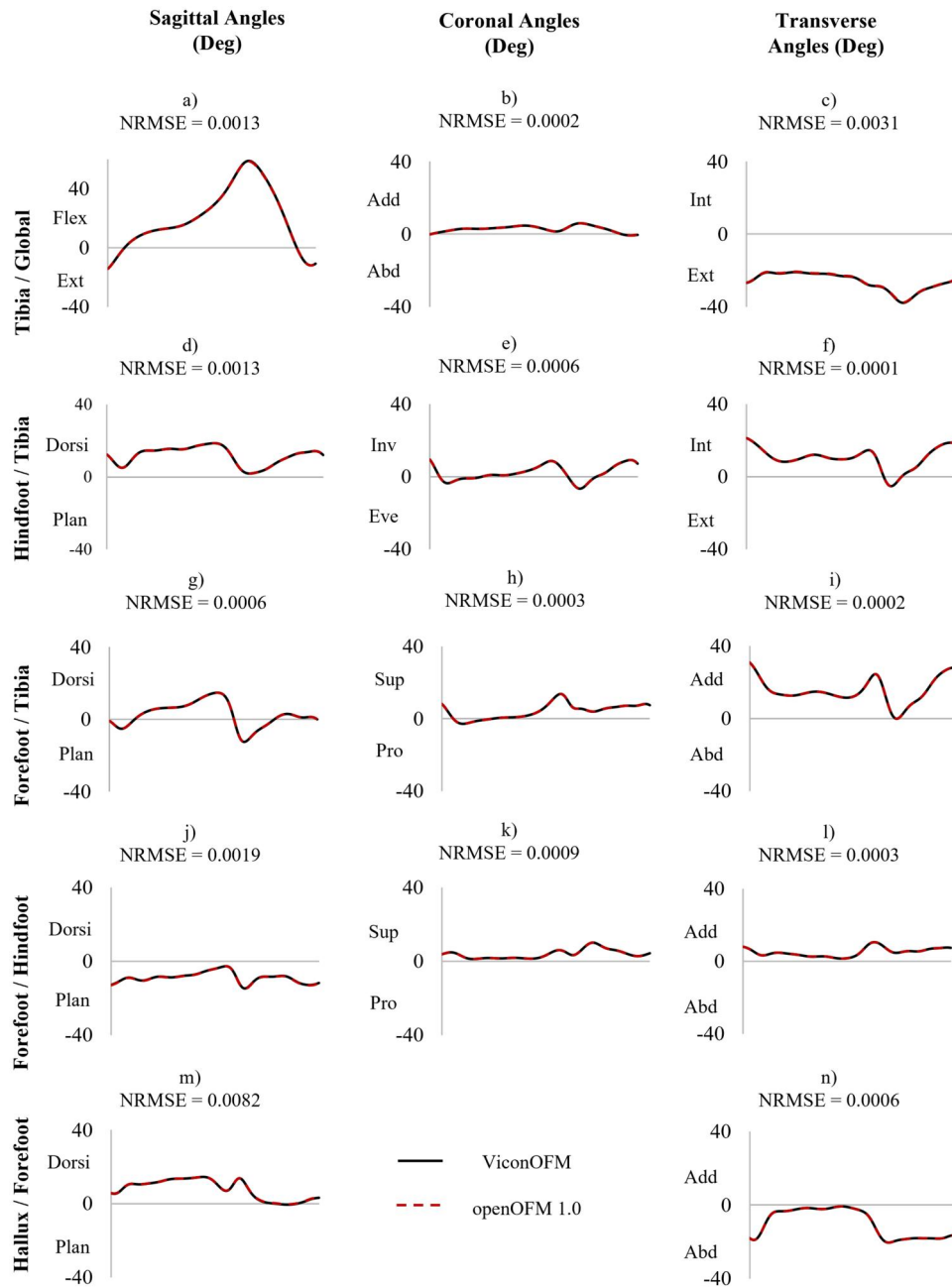


Figure 4. Tibia/global, hindfoot/tibia and forefoot/tibia forefoot/hindfoot and hallux/forefoot angles (right side) in Vicon processed OFM and openOFMv1.0 for a representative trial of healthy gait (participant H). The sagittal plane angles are flexion/extension (flex/ext) and dorsiflexion/plantarflexion (dorsi/plan). The coronal plane angles are adduction/abduction (add/abd), inversion/eversion (inv/eve), and supination/pronation (sup/pro). Finally, the transverse plane angles are internal/external (int/ext) rotation, and adduction abduction (add/abd).

3. Results

3.1. Version 1.0

The Python (v3.11) implementation of the openOFM v1.0 and the OFM plug-in from Vicon Nexus (Vicon Nexus version 2.11.0.127963h x86) were compared using the NRMSE between outputs. In healthy gait, the default Vicon settings (HFFlat = *False*, UseFloorFF = *False*) were used to compare the two models. In

healthy gait, the three-dimensional joint kinematics for the hindfoot/tibia, hallux/forefoot and forefoot/hindfoot angles showed an NRMSE of up to 0.0083 (Figure 4). Similarly, global (tibia/global) and non-contiguous segment (forefoot/tibia) angles revealed an NRMSE inferior to 0.0031 (Figure 4). For the healthy subject, the results showed similar agreement if the previously mentioned settings were both set to true. These results were similar for pathological gait,

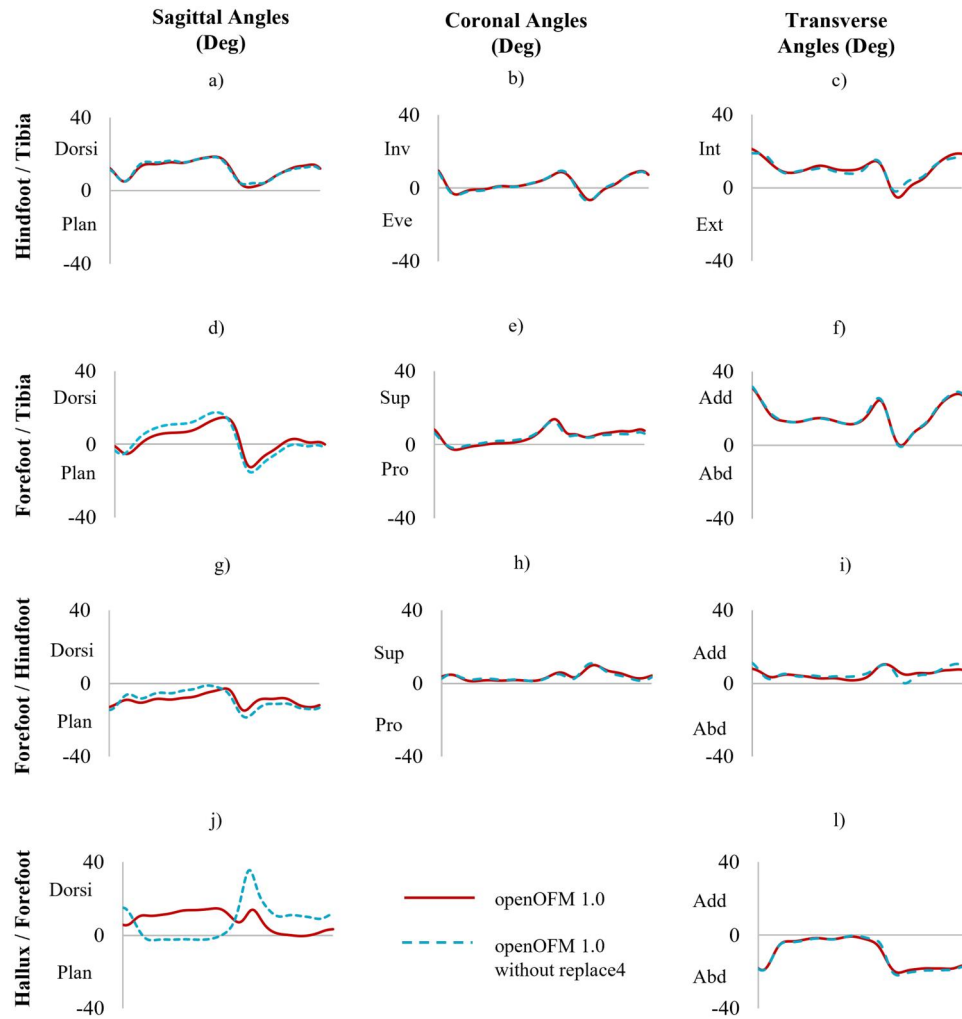


Figure 5. Hindfoot/tibia, forefoot/tibia, forefoot/hindfoot, hallux/forefoot angles (right side) in openOFMv1.0 with and without *replace4* in healthy gait (participant H). The sagittal plane angles are flexion/extension (flex/ext) and dorsiflexion/plantarflexion (dorsi/plan). The coronal plane angles are adduction/abduction (add/abd), inversion/eversion (inv/eve), and supination/pronation (sup/pro). Finally, the transverse plane angles are internal/external (int/ext) rotation, and adduction abduction (add/abd).

with an average NRMSE of 0.0012 in the database previously presented in Table 1. Finally, arch height index results had an average NRMSE of 0.0074 and 0.045 for the right and left side, respectively.

3.2. Version 1.1

In version 1.1, the following changes are made: *replace4* is no longer used, a single tibia segment is defined using OFM markers only, the *Hindfoot Flat* function and local coordinate system labels are modified, and the hallux local coordinate system definition is modified.

The effect of *replace4* (Section 2.2.2) is shown in healthy gait in Figure 5. The largest effects are seen in the hallux/forefoot angles, with peak dorsiflexion at push off increased without the use of *replace4*. Another example of the effect of *replace4* in pathological gait shown in Supplementary Figure D9 mostly reveals

changes in the sagittal (forefoot/tibia, forefoot/hindfoot, and hallux/forefoot) and coronal (forefoot/tibia) planes. Each modification introduced in v1.1 was then evaluated in isolation, without the use of *replace4*. This was done using a representative trial, for relevant inter-segment kinematics on the right side.

The impact of the modifications to the tibia segment presented in Section 2.3.2 are illustrated in healthy gait by comparing the angles obtained in openOFMv1.0 (without *replace4*) and openOFMv1.1 (Figure 6). The most noticeable differences are observed in the transverse plane.

The minimal impacts of the modifications to the *Hindfoot Flat* function (Section 2.2.4) are illustrated in a representative trial from a patient with a planus right foot (Figure 7).

The modifications made to labelling of local coordinate systems had no impact on kinematics results, and are solely for communication purposes (Figure 2).

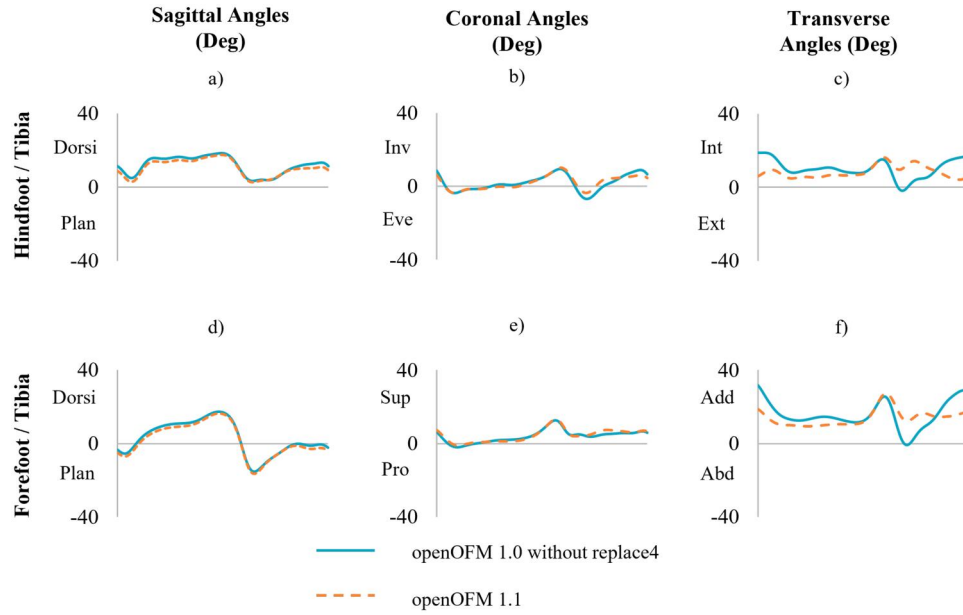


Figure 6. Hindfoot/tibia and forefoot/tibia angles (right side) in openOFMv1.0 (without *replace4*) and openOFMv1.1 for a representative trial in pathological gait (participant P3). The sagittal plane angles are flexion/extension (flex/ext) and dorsiflexion/plantarflexion (dorsi/plan). The coronal plane angles are adduction/abduction (add/abd), inversion/eversion (inv/eve), and supination/pronation (sup/pro). Finally, the transverse plane angles are internal/external (int/ext) rotation, and adduction abduction (add/abd).

The modifications made to the hallux definition have no effect on sagittal and transverse plane angles, frontal plane angles are always zero.

4. Discussion

4.1. Summary

This manuscript details the development of an open-source version of the OFM (openOFM). We achieved the aims of our study. First, we were able to reproduce the commercial implementation of the OFM (version 1.0). In healthy gait, the three-dimensional joint kinematics for the hindfoot/tibia, hallux/forefoot and forefoot/hindfoot, as well as global (tibia/global) angles, non-contiguous segment (forefoot/tibia) angles, and arch height index of openOFM showed strong agreement with the Vicon implementation, irrespective of the processing settings used. The agreement between the implementations remained equally satisfactory in pathological gait. Second, we identified inconsistencies between the commercial implementation and the original descriptions from Carson et al. (Carson et al. 2001) and Stebbins et al. (Stebbins et al. 2006) revealing their impact on resulting kinematics and implemented them in openOFM version 1.1. The largest differences are due to an integrated smoothing and gap filling function (*replace4*), introduced by Stebbins et al. in 2006 (Stebbins et al. 2006). In

addition, the implementation of a tibia segment based only on OFM markers as in Carson et al. (Carson et al. 2001), introduces differences in transverse plane angles involving the tibia. Finally, there are minimal differences due to the modifications made in the *Hindfoot Flat* function to better reflect the flat hindfoot assumptions in Stebbins et al. (Stebbins et al. 2006). In version 1.1, for increased fidelity to the model description by Carson et al. (Carson et al. 2001), local coordinate segment labels are changed and the hallux local coordinate system is rotated with respect to its definition in version 1.0. These modifications have no impact on model outputs.

4.2. Relevance and contributions

The original OFM code was developed for in-house staff and was not shared publicly. We addressed this underlying issue, providing both mathematical descriptions and open source code *via* our openOFM project. Moreover, we highlighted the role of the *replace4* function which was embedded in the commercial implementation to provide a basic compensation for potential marker gaps. As marker gaps are now greatly reduced due to improved motion capture hardware and more easily removed ('filled') using advanced processing, the function is removed in version 1.1. Our analyses show noticeable and variable sensitivity to this

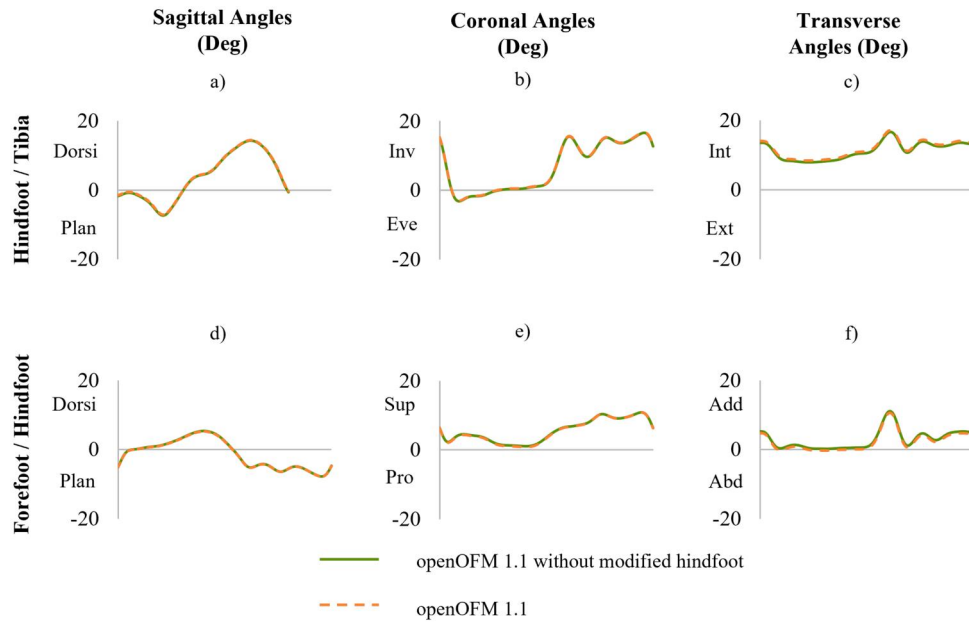


Figure 7. Hindfoot/tibia and forefoot/hindfoot angles (right side) in openOFMv1.1 with (dotted line) and without (solid line) the modified *Hindfoot Flat* definition for a participant with a planus right foot (P3). The sagittal plane angles are flexion/extension (flex/ext) and dorsiflexion/plantarflexion (dorsi/plan). The coronal plane angles are adduction/abduction (add/abd), inversion/eversion (inv/eve), and supination/pronation (sup/pro). Finally, the transverse plane angles are internal/external (int/ext) rotation, and adduction abduction (add/abd).

function (Figures 5 and Supplementary Figure D9), particularly in the forefoot, which is known to be flexible (Chan et al., 2019). The openOFM will allow exploration of better compensation algorithms for this flexibility.

Comparable work by Leboeuf et al. in 2019 (Leboeuf et al. 2019), developing a Python implementation (PyCGM2 project) of the popular Plug-in-Gait model available in Vicon Nexus, found a root mean square error (RMSE) between their implementation and the Vicon version of up to 0.04° . We chose to report normalized values; however, without normalization, our results reveal an average RMSE of 0.03° and maximum RMSE in the foot of 0.04° , suggesting comparable accuracy.

The open-source nature of this project will increase the accessibility of the OFM for both researchers and clinicians, allowing more widespread use of the OFM and independent validation and investigation of the model by the biomechanics community. It will allow the model to be more easily adapted to different foot pathologies; for example when deformity affects where markers can be placed or when the tracking of different or additional foot segments is required. This in turn will improve the quality and reliability of multi-segment foot modelling, providing higher quality information on foot motion to inform foot health and function.

4.3. Limitations

Some limitations of this study warrant discussion. First, the sample size was small making it difficult to draw conclusions on potential differences that could be observed across populations when using the two model versions. Here, we only included a group of patients with heterogeneous foot pathologies to ‘stress test’ the various functions in the code for resilience and reveal some of its behaviours in unique populations. Second, we have not validated either model against underlying bone motions. Our open-source code could make such investigations by other research groups more feasible in the future.

4.4. Usage notes and future directions

In openOFM version 1.0 (and the current commercial implementation), the hindfoot/tibia and forefoot/tibia kinematics are highly dependent on lower body processing of the Plug-in Gait model and how static offsets for tibial torsion are implemented in the static trial (Lower body kinematics – Nexus 2.16 documentation 2024) for the tibial anatomical frame (Section 2.2.1 (Supplementary Figure D8)). Special consideration should be given to the method employed for tibial segment definition when analysing hindfoot/tibia kinematics.

The differences between the two versions of the openOFM require more detailed evaluation. More specifically, further investigation into the effects of the original *Hindfoot Flat* function in cases of pathological inversion-eversion of the hindfoot could be of interest. The updated definition of the function appears to be more robust; however, its application should be extended to cases where the hindfoot is not flat, with a supporting surface that can be used as a reference plane in place of the floor to increase repeatability of results in all use cases. These differences highlight the need to consider the version used when interpreting OFM results. Basing interpretations on the original OFM publications (Carson et al. 2001; Stebbins et al. 2006) when analysing results obtained from the Vicon OFM may lead to inaccurate conclusions.

A priority when developing future versions of the openOFM is backwards compatibility, allowing those who have previously used the OFM to reprocess data using the newest version of the model and compare the outputs. This is especially important for users working in clinical gait analysis settings. The placement of existing markers should not be changed, and the use of any new markers should be optional.

Some of the planned improvements include the following. Given the sensitivity of the hindfoot markers to misplacement (Carty et al. 2015), a method for correcting the hindfoot plantar surface when the hindfoot is not flat on the floor is needed. It is also our aim to provide an improved measure of the medial longitudinal arch behaviour (Uhan et al. 2023), a medio-lateral division of the forefoot (metatarsals), and a method to correct the plantar surface of the hindfoot when the hindfoot is not flat on the floor. Finally, additional measures specific to the evaluation of particular foot pathologies may be of interest.

5. Conclusion

The openOFM project provides an accurate open-source implementation of the commercial OFM. The process of re-coding the OFM has brought to light some discrepancies in the published definitions and implementation of the model that, whilst small, needed to be addressed. This project presents an initial evaluation of these discrepancies, while allowing independent investigation by the community.

Acknowledgements

All authors acknowledge the contributions of Ariane Lavoie-Boutin, Aurianne Coulomb, and Achraf Kabbabi to initial code developments.

CRedit authorship statement

Philippe C. Dixon: Conceptualization, data curation, funding acquisition, methodology, project administration, resources, software, supervision, validation, visualization, writing – original draft, writing – review and editing. **Elodie E. Drew:** Data curation, formal analysis, investigation, methodology, software, validation, visualization, writing – original draft, writing – review and editing. **Sean P. McBride:** Data curation, formal analysis, investigation, methodology, project administration, resources, software, supervision, visualization, writing – review and editing. **Marian Harrington:** Data curation, methodology, resources, supervision, validation, writing – review and editing. **Julie Stebbins:** Methodology, resources, supervision, validation, writing – review and editing. **Amy B. Zavatsky:** Methodology, resources, supervision, validation, writing – review and editing.

Disclosure statement

No potential conflict of interest was reported by the author(s).

Funding

This work was supported by the MUSCO foundation. Elodie E. Drew is supported by a Fonds de recherche du Québec (FRQ) scholarship. Philippe C Dixon acknowledges support from the (FRQ) Junior 1 research scholar award.

ORCID

Philippe C. Dixon  <http://orcid.org/0000-0003-3581-7259>
 Elodie E. Drew  <http://orcid.org/0009-0001-1461-4308>
 Marian Harrington  <http://orcid.org/0000-0002-7454-1104>
 Julie Stebbins  <http://orcid.org/0000-0001-6496-8588>
 Amy B. Zavatsky  <http://orcid.org/0000-0002-9618-286X>

Data availability statement

The openOFM is available for download for use in Matlab, Python, and Vicon Nexus at <https://github.com/McGillMotionLab/openOFM>. Pipelines for Vicon Nexus applications are also provided. The validation data from the healthy subject presented in Table 1 is also shared on GitHub, in the *Data_Validate* folder. The following software versions were used for development: Matlab R2023a, Python 3.11.4, Vicon Nexus 2.15. A step-by-step user guide is shared in Supplementary Appendix E.

References

- Ahmed Z, Kinjol FJ, Ananya IJ. 2021. Comparative analysis of six programming languages based on readability, writability, and reliability. 2021 24th International Conference on Computer and Information Technology (ICCIT). p. 1–6.

- Bishop C, Paul G, Thewlis D. 2012. Recommendations for the reporting of foot and ankle models. *J Biomech.* 45(13):2185–2194. doi: [10.1016/j.jbiomech.2012.06.019](https://doi.org/10.1016/j.jbiomech.2012.06.019).
- Carson MC, Harrington ME, Thompson N, O'Connor JJ, Theologis TN. 2001. Kinematic analysis of a multi-segment foot model for research and clinical applications: a repeatability analysis. *J Biomech.* 34(10):1299–1307. doi: [10.1016/S0021-9290\(01\)00101-4](https://doi.org/10.1016/S0021-9290(01)00101-4).
- Carty CP, Walsh HPJ, Gillett JG. 2015. Sensitivity of the Oxford Foot Model to marker misplacement: a systematic single-case investigation. *Gait Posture.* 42(3):398–401. doi: [10.1016/j.gaitpost.2015.06.189](https://doi.org/10.1016/j.gaitpost.2015.06.189).
- Chan P-H, Stebbins J, Zavatsky AB. 2019. Marker cluster rigidity in a multi-segment foot model. *J. Biomech.* 84: 284–289. doi: [10.1016/j.jbiomech.2018.12.045](https://doi.org/10.1016/j.jbiomech.2018.12.045).
- Fuller DA, Keenan MAE, Esquenazi A, Whyte J, Mayer NH, Fidler-Sheppard R. 2002. The impact of instrumented gait analysis on surgical planning: treatment of spastic equinovarus deformity of the foot and ankle. *Foot Ankle Int.* 23(8):738–743. doi: [10.1177/107110070202300810](https://doi.org/10.1177/107110070202300810).
- Grood ES, Suntay WJ. 1983. A joint coordinate system for the clinical description of three-dimensional motions: application to the knee. *J Biomech Eng.* 105(2):136–144. doi: [10.1115/1.3138397](https://doi.org/10.1115/1.3138397).
- Kadaba MP, Ramakrishnan HK, Wootten ME. 1990. Measurement of lower extremity kinematics during level walking. *J Orthop Res.* 8(3):383–392. doi: [10.1002/jor.1100080310](https://doi.org/10.1002/jor.1100080310).
- Kidder S, Abuzzahab F, Harris G, Johnson J. 1996. A system for the analysis of foot and ankle kinematics during gait. *IEEE Trans Rehabil Eng.* 4(1):25–32. doi: [10.1109/86.486054](https://doi.org/10.1109/86.486054).
- Leardini A, Benedetti MG, Berti L, Bettinelli D, Natio R, Giannini S. 2007. Rear-foot, mid-foot and fore-foot motion during the stance phase of gait. *Gait Posture.* 25(3):453–462. doi: [10.1016/j.gaitpost.2006.05.017](https://doi.org/10.1016/j.gaitpost.2006.05.017).
- Leardini A, Caravaggi P, Theologis T, Stebbins J. 2019. Multi-segment foot models and their use in clinical populations. *Gait Posture.* 69:50–59. doi: [10.1016/j.gaitpost.2019.01.022](https://doi.org/10.1016/j.gaitpost.2019.01.022).
- Leboeuf F, Baker R, Barré A, Reay J, Jones R, Sangeux M. 2019. The conventional gait model, an open-source implementation that reproduces the past but prepares for the future. *Gait Posture.* 69(2019):235–241. doi: [10.1016/j.gaitpost.2019.04.015](https://doi.org/10.1016/j.gaitpost.2019.04.015).
- Mesirov JP. 2010. Accessible reproducible research. *Science.* 327(5964):415–416. doi: [10.1126/science.1179653](https://doi.org/10.1126/science.1179653).
- Michaud B, Begon M. 2021. Ezc3d: an easy c3d file I/O cross-platform solution for C++, python and matlab. *JOSS.* 6(58):2911. doi: [10.21105/joss.02911](https://doi.org/10.21105/joss.02911).
- Pires, Nev. 2020. Replace 4 Macro. by Vicon | Motion Capture Software. <https://www.vicon.com/software/models-and-scripts/replace-4-macro/>.
- Pothrat C, Authier G, Viehweger E, Berton E, Rao G. 2015. One- and multi-segment foot models lead to opposite results on ankle joint kinematics during gait: implications for clinical assessment. *Clin Biomech.* 30(5):493–499. doi: [10.1016/j.clinbiomech.2015.03.004](https://doi.org/10.1016/j.clinbiomech.2015.03.004).
- Schallig W, van den Noort JC, McCahill J, Stebbins J, Leardini A, Maas M, Harlaar J, van der Krogt MM. 2020. Comparing the kinematic output of the Oxford and Rizzoli Foot Models during normal gait and voluntary pathological gait in. *Gait Posture.* 82(2020):126–132. doi: [10.1016/J.GAITPOST.2020.08.126](https://doi.org/10.1016/J.GAITPOST.2020.08.126).
- Schallig W, van den Noort JC, Piening M, Streekstra GJ, Maas M, van der Krogt MM, Harlaar J. 2022. The Amsterdam Foot Model: a clinically informed multi-segment foot model developed to minimize measurement errors in foot kinematics. *J Foot Ankle Res.* 15(1):46. doi: [10.1186/s13047-022-00543-6](https://doi.org/10.1186/s13047-022-00543-6).
- Schwartz M, Dixon PC. 2018, January. The effect of subject measurement error on joint kinematics in the conventional gait model: insights from the open-source pyCGM tool using high performance computing methods. *PLOS One.* 13(1):e0189984. doi: [10.1371/journal.pone.0189984](https://doi.org/10.1371/journal.pone.0189984).
- Stebbins J, Harrington M, Thompson N, Zavatsky A, Theologis T. 2006. Repeatability of a model for measuring multi-segment foot kinematics in children. *Gait Posture.* 23(4):401–410. doi: [10.1016/j.gaitpost.2005.03.002](https://doi.org/10.1016/j.gaitpost.2005.03.002).
- Uhan J, Kothari A, Zavatsky A, Stebbins J. 2023. Using surface markers to describe the kinematics of the medial longitudinal arch. *Gait Posture.* 102(2023):118–124. doi: [10.1016/j.gaitpost.2023.03.016](https://doi.org/10.1016/j.gaitpost.2023.03.016).
- Vicon. 2010. Body Builder. | Vicon | Motion Capture Software. <https://www.vicon.com/software/bodybuilder/>.
- Vicon. 2024. Lower body kinematics – Nexus 2.16 documentation. Vicon Help. <https://help.vicon.com/space/Nexus216/11606631/Lower+body+kinematics#DynamicKJC>.